Journal of ELECTRONIC MATERIALS, Vol. 50, No. 4, 2021
https://doi.org/10.1007/s11664-020-08662-1

ASIAN CONSORTIUM ACCMS–INTERNATIONAL CONFERENCE ICMG 2020

Comprehensive Study and Realizing an Enhanced Efficiency of the Thermoelectric Generator Along with Its Thermomechanical Properties

SUHASINI SATHIYAMOORTHY,[1] R. KUMAR,[1,5] BERNAURDSHAW NEPPOLIAN,[2] DHANALAKSHMI SAMIAPPAN,[1] SURYA PRATAP SINGH,[1,3] SUMEDHA ROY,[1,3] NIKHIL DWIVEDI,[1,3] and PANDIYARASAN VELUSWAMY[3,4,6]

1.—Department of Electronics and Communication Engineering, SRM Institute of Science and Technology, Kattankulathur, Tamil Nadu 603203, India. 2.—SRM Research Institute, SRM Institute of Science and Technology, Kattankulathur, Chennai, Tamil Nadu 603203, India. 3.—Smart and Innovative Laboratory for Energy Devices (SMILE), Indian Institute of Information Technology Design and Manufacturing (IIITDM) Kancheepuram, Chennai 600127, India. 4.—Department of Electronics and Communication Engineering, Indian Institute of Information Technology Design and Manufacturing (IIITDM) Kancheepuram, Chennai 600127, India. 5.—e-mail: kumarr@srmist.edu.in. 6.—e-mail: pandiyarasan@yahoo.co.in

This paper proposes a real-time simulation model to simplify the research and outcome of a portable thermoelectric generator (TEG) system in real conditions. Consequently, the model is divided into three parts: conventional, segmented, and hybrid TEG systems. The conventional TEG system consisted of Bi_2Te_3 as the *p*-type and the *n*-type materials, whereas the segmented and the hybrid TEG systems consisted of a different combination of materials, including PbTe and Sb_2Te_3. The optimization of the TEG system length was carried out to achieve the highest power output, which was found to be 2 mm. In addition, thermomechanical stress distribution analysis of the module was conducted to determine the maximum load the TEG system could withstand before undergoing fracture, depending upon the yield strength of the material. The stress was analyzed in all three TEG systems, and the results were evaluated. Results were observed from the optimized length at 2 mm. The conventional, segmented, and hybrid TEG systems showed maximum power output of 147.122 mW, 171.934 mW, and 550 mW, respectively, with a temperature difference at 50 K.

Key words: Thermoelectric generators, electric potential, hybrid structure, von Mises

INTRODUCTION

Over the past decade, portable device technology has transformed the world and has become an essential part of our lives, with devices that are thin and lightweight, making them easy to carry and hold. These devices are incredibly small and have relatively high storage, smaller processing chipsets, and longer battery life. However, battery power plays a vital role in portable devices, which makes a device that can operate longer between charges more desirable. Battery technology has not advanced in decades; the battery has to be charged or replaced at regular intervals. But we are on the verge of a power revolution as the need for batteries increases. Thus new battery technology must be

(Received July 25, 2020; accepted December 1, 2020; published online January 4, 2021)

developed for portable devices to produce batteries that are smaller and are able to hold a charge longer.[1–3]

To overcome the problem of battery charging, renewable energy has been explored as an alternative energy source, including solar energy, wind power, hydropower, friction charging, and thermoelectric power generation.[4–6] However, the fast-growing demand for power generation systems is focused on portable devices of a specific size with a range of application considerations, such as solar and thermoelectric in general. The intent is to address the need for solar power generation due to climate change. Still, the contribution of thermoelectric sources of power from waste heat and the associated benefits are enormous.[7] This is due to the Seebeck effect: if there is a temperature difference between the two ends of such material, current can start to flow, and electrical voltage can be generated. Thermoelectric material is most suitable for developing power generators because it can promote high reliability, has a long operating lifetime, has no moving parts and no noise, is easily maintained, and is environmentally friendly. The thermoelectric conversion efficiency of a thermoelectric device is governed by the dimensionless figure of merit $ZT = S^2\sigma/\kappa\, T$, where σ is the electrical conductivity, S is the Seebeck coefficient, κ is the thermal conductivity, T is the absolute temperature, and $S^2\sigma$ is the power factor. In order to obtain better efficiency, the materials should have high electrical conductivity, a high Seebeck coefficient, and low thermal conductivity.[8]

Importantly, the new technology is a continuous iteration of the portable device power improvements using thermoelectric material and temperature gradients to generate electricity, so power can be generated using human body heat. Human skin is considered as the hot side of a wearable thermoelectric device (WTED), whereas the ambient temperature functions as the cold side. A WTED consists of a pair of *p*-type and *n*-type semiconductor legs placed between the hot and cold surfaces. The *p*-type leg material has a positive Seebeck coefficient because it consists of a large number of holes; similarly, the *n*-type leg material has a negative Seebeck coefficient, and the electrodes play an essential role in WTED schematic modules, as shown in Fig. 1a, with higher conductivity necessary in order to achieve higher output and efficiency.[9]

Recently, there has been growing interest in achieving high energy conversion efficiency at low cost, which can deliver precise output efficiency by optimization of the thermoelectric materials and thermoelectric generator geometry.[10] Asides were improving the ZT of materials; in particular, optimizing the geometry of a thermoelectric generator module is a way to enhance its efficiency and power output. To date, the creation of complex thermoelectric materials with an improved figure of merit can be characterized into three categories, namely semiconductors, ceramics including metal oxides, and polymers and their composites.[11] In Ref.,[12] materials that obtain the highest figure of merit efficiency of a thermoelectric device are Bi, Te, Pb, Sb, and Se.

Yongming et al.[13] developed a theoretical three-dimensional numerical model to optimize the geometry of thermoelectric legs, and the number of pairs can also enhance the output efficiency. They argued that geometry optimization is significant for high thermoelectric power generation. The geometric optimization of height, cross-sectional area, and increased array of legs has also been applied successfully to improve the overall performance and reduce cost. Results have shown that by changing the height of the thermoelectric pair from 0.5 mm to 5 mm, the voltage obviously increases, although the current varies only 0.15 mA; on the other hand, changing the area of thermoelectric pairs from 0.4×0.4 mm^2 to 2.2×2.2 mm^2 decreases the voltage apparently with the current varying by only 0.651 mA. Similarly, the array of thermoelectric pairs increased from 7 to 199, the voltage varies up to 1.75 mV; however, the current decreases obviously. On the contrary, the highest figure of merit belongs to the ideal situation, taller height, more significant cross-sectional area, and the number of thermoelectric pairs.

Samson et al.[14] studied the influence of the thermoelectric and mechanical performance of a segmented device using finite element analysis. The effects of the proposed segmented geometry on the performance of annular thermoelectric generators and non-segmented annular thermoelectric generators were studied using COMSOL 5.3 Multiphysics software for the numerical simulation of thermo-mechanical properties. Bismuth telluride and cobalt/antimony material with maximum operating temperatures of 498 K and 798 K were used as the cold and hot segments, respectively. The efficiency with and without von Mises stress in the legs was 21.7% and 35.4% for bismuth telluride with a temperature difference of 200 K. The increased thermoelectric leg length led to a decrease in thermal stress, with an increase in mechanical reliability and a reduction in electrical performance.

Constantinos et al.[15] reported the design of high-efficiency segmented thermoelectric generators using computational and analytical modeling. Initially, the experiment was performed for homogeneous Bi_2Te_3 and PbTe materials with a heat source and heat exchanger thermal resistance, which increased the performance of the segmented thermoelectric generator system with an increase in the temperature gradient. The computational results indicated excellent temperature distribution across the thermoelectric generator legs. The accuracy of the analytical modeling was also improved—the proposed segmented thermoelectric generator

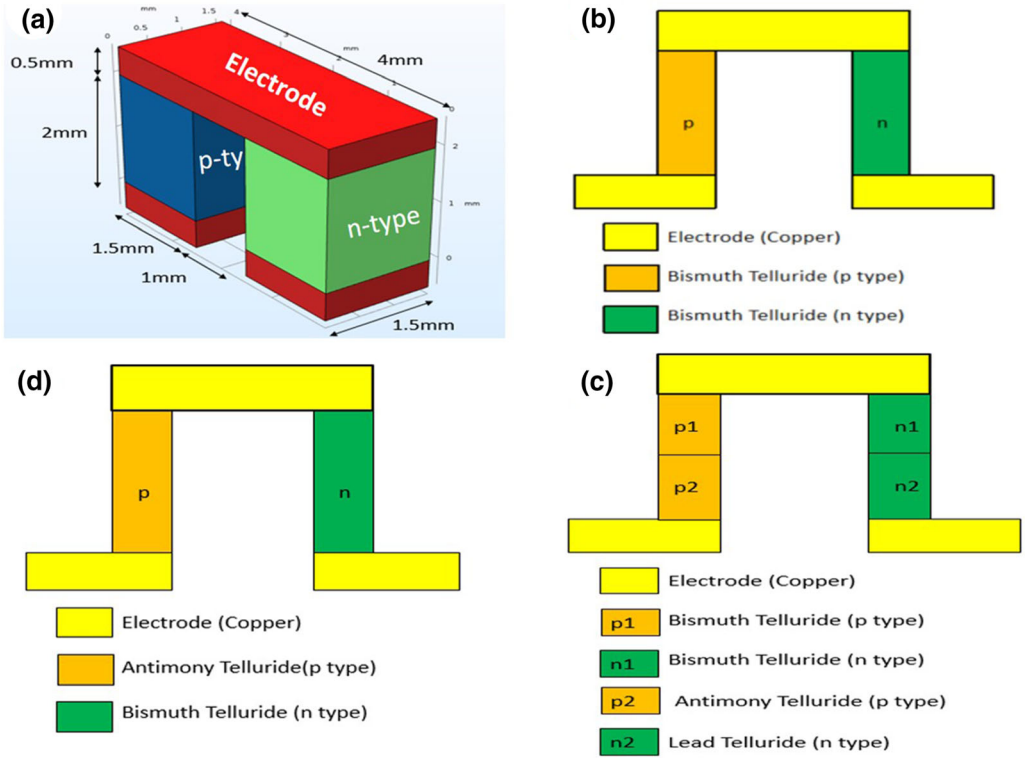

Fig. 1. Schematic geometry of a two-leg thermoelectric device considering the (a) boundary conditions. (b) Conventional, (c) segmented, and (d) hybrid TEG systems.

demonstrated efficiency of 5.29% for a temperature gradient of 324.6 K.

The value of optimizing the geometry of a wearable thermoelectric device (WTED) with an optimal temperature range for a large temperature gradient along the axial direction was found based on a detailed literature survey. Moreover, it was observed that the segmented conventional thermoelectric generator obtains higher output power. In this present work, we investigated the influence of three-dimensional (3D) temperature and voltage distributions, which are illustrated in detail, concerning the mechanical stress analysis to enhance the performance of a thermoelectric generator. To the best of our knowledge, this study is the first of its kind. It will provide valuable information on the potential model description of hybrid materials of *p*-type and *n*-type legs regarding their mechanical behaviors. Further, the external load is studied in depth using COMSOL Multiphysics software.

METHODOLOGY

Structural Description and Material Selection

A schematic representation of the thermoelectric generator with geometrical dimensions is presented in Fig. 1a. It consists of a semiconducting material such as *p*-type and *n*-type legs sandwiched by the electrode, which helps to reduce the thermal stress in the device. In the thermoelectric generator, the length, width, and depth of the elements are 1.5 mm, 1.5 mm, and 2 mm, respectively, with a 1-mm spacing, and the thickness of the electrodes is 0.5 mm. The properties of the materials, including the electrical resistance, thermal conductivity, Seebeck coefficient of the TEG system, and resistance of the electrodes, are given in Table I. For a better understanding and simplicity of solving the structural problem, the following assumptions are adopted:

1. The material properties of the *p*-type and *n*-type elements are identical and temperature-dependent.
2. The stimulation is performed for the pair of *p*-type and *n*-type elements.[16]
3. The lateral surface of the heat transfer in the element surface is ignored.
4. If the thermoelectric element length is greater than 200 μm, then the resistance between the electrode and elements can be neglected.[17]

Physical Model

The 3D geometries studied and their materials are represented in Fig. 1, including (a) boundary conditions, and (b) conventional, (c) segmented, and (d) hybrid thermoelectric generators (TEG), for the numerical simulation. It constituted a pair of *p*- and *n*-type legs and ensured the electrical contact as a copper layer between the legs. In a conventional

Table I. Properties of different TE materials at room temperature (300 K)

Material	Seebeck coefficient (μVK^{-1})	Thermal conductivity ($Wm^{-1}K^{-1}$)	Electrical conductivity (Sm^{-1})
Bismuth telluride ($Bi_2Te_{3)}$ *p*-type	200	1.15	5.08×10^4
Bismuth telluride (Bi_2Te_3) *n*-type	−200	1.15	5.08×10^4
Lead telluride (PbTe) *p*-type	187	1.46	6.10×10^4
Lead telluride (PbTe) *n*-type	−187	1.46	6.10×10^4
Antimony telluride (Sb_2Te_3) *p*-type	209	1.80	9.26×10^4
Antimony telluride (Sb_2Te_3) *n*-type	−209	1.80	9.26×10^4

TEG, low-temperature material Bi_2Te_3 for the two legs present the best thermoelectric device, allowing one leg to be considered a *p* type and the other an *n* type with their difference being the signal of the Seebeck coefficient. The legs are connected electrically in series and thermally in parallel. If the functional temperature range goes higher, there is no single material that will be regime. At low temperatures, Bi_2Te_3 was chosen due to its higher figure of merit. In contrast, with high temperature, other combinations of TEG materials, such as Sb_2Te_3 and PbTe, utilized in the segmented TEG are arranged according to their optimal operating temperature range, from high to low. In this sense, herein, we propose a hybrid architecture aligned with two dissimilar materials, such as Bi_2Te_3, Sb_2Te_3, and PbTe for the *p*-type and *n*-type thermoelectric materials.

Boundary Conditions and Governing Equations

To simplify the analysis, some primary boundary conditions established for the thermoelectric generator model are listed below.

- The heat transfer module is used for the evaluation of temperature gradient in the TEG by the forced conduction and convection with the surface-to-surface temperature distribution.
- Steady-state conditions are assumed for the thermoelectric modules; the specific temperature is considered as a hot side, and the thermoelectric module is cold.
- An adiabatic condition is assumed on the surface of the TEG, with no heat losses from other surfaces.
- In the TEG, a heat flux of about 300 K to 350 K is applied on the top surface, while the bottom surface is kept constant at 300 K, with the highest temperature gradient of 50 K.
- A unified mesh has been considered in our module to define Ohm's law and other electrical and thermomechanical properties.

Utilizing a multi-physics model of a thermoelectric module evaluated using COMSOL, the numerical calculation involving electric potential, resistance, and power has been studied using the following governing equations:

1. The formula for open-circuit voltage (electric potential) is expressed as

$$V_{oc} = N \int_{T_c}^{T_h} (Sp - Sn) dT \tag{1}$$

where V_{oc} is the open-circuit voltage, N is the number of legs in the thermoelectric module, T_c is the temperature on the cold surface, T_h is defined as the temperature on the hot side of the module,Sp is the Seebeck coefficient of the *p*-type material, and Sn is the Seebeck coefficient of the *n*-type material.

2. The internal resistance of the thermoelectric module is given by

$$R = n\left(\rho_p L_p (A_p)^{-1} + \rho_n L_n (A_n)^{-1}\right) \tag{2}$$

3. The equivalent thermal conductivity is given by:

$$K = n\left(k_p A_p (L_p)^{-1} + k_n A_n (L_n)^{-1}\right) \tag{3}$$

where R is the internal resistance of the thermoelectric material, L is the length of the thermoelectric leg, A is the cross-sectional area of the

thermoelectric module, and ρp and ρn are the electrical resistivity of the p-type and the n-type legs, respectively. k is the thermal conductivity of each leg.

4. The power of the thermoelectric module is given by:

$$P = \frac{V_{OC}^2}{4R} \tag{4}$$

Optimization of Legs

The geometry optimization of thermoelectric legs and the number of pairs can also enhance the thermoelectric output efficiency. In this, the geometry optimization of leg height would increase the output voltage according to the temperature gradients, as shown in Fig. 2a. The outcome indicates an adjustment in the height of the thermoelectric pair from 2 mm to 3 mm; the voltage increases with respect to variations in temperature. This shows that expanding the TEG leg length can improve the mechanical reliability yet decrease the electrical performance of the TEG system.[7,18,19] On the other hand, a height of 2 mm with 26 pairs of TEGs was used for further numerical simulation purposes. Thus, a thermal gradient imposed on an array of bismuth telluride is the result of a potential generation across the surface of the TEG system, as shown in Fig. 2b. The temperature and electrical potential distribution contour plots are presented graphically in Fig. 2c, d. the maximum output voltage was produced around 3000 mV with the temperature gradient of 50 K, although the current varies only 0.15 mA through the load resistance as given by Eqs. 1–3.

RESULTS AND DISCUSSION

In this section, a detailed analysis is presented, and the results of thermoelectric and mechanical performance are shown. Firstly, the parametric optimization study was followed by the selection of the number of legs. Furthermore, a conventional and segmented system is given for the essential parameters influencing the TEG performance. Finally, a comparison of the hybrid effects on TEG performance is presented using COMSOL Multiphysics under the heat transfer in the interface of the solid. Figure 2 shows the temperature distribution of a thermoelectric system, which illustrates that the temperature flows from the hot side to the cold side of the TEG system as conduction takes place. The electrical potential is otherwise called the open-circuit voltage, which is a progressively essential boundary for deciding the force acquired from the TEG. It is seen that as the temperature gradient steps up between the hot

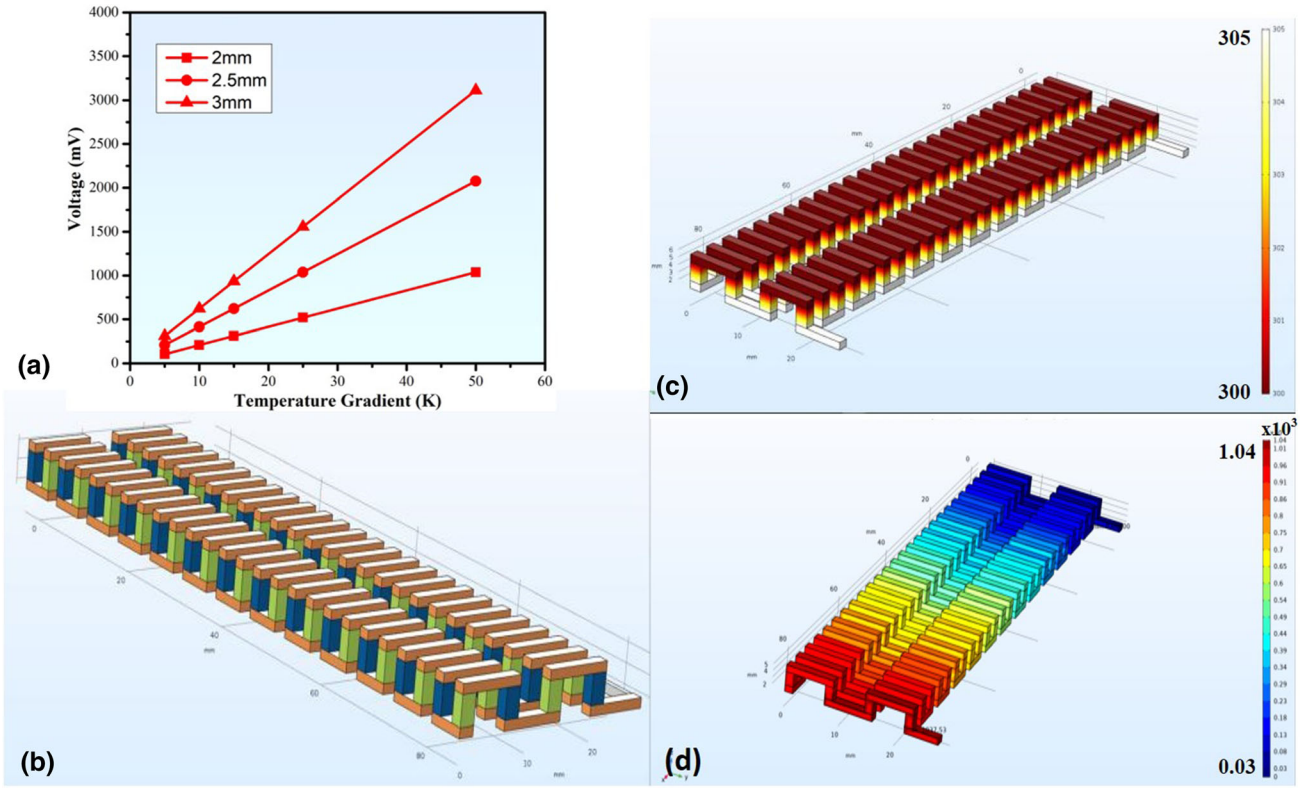

Fig. 2. (a) Variation of leg length with temperature gradient, schematic diagram of a three-dimensional cross-section view of the (b) array of leg pairs, (c) temperature distribution, and (d) imposition of electric potential distribution on the TEG legs.

side and cold side of the system, the open-circuit voltage also increases. This is known as the Seebeck effect, which is to develop an output voltage increase. A temperature gradient of about 50 K in the TEG system was considered as the maximum temperature range in this WTED.

Utilizing the conventional 52 legs of the TEG system, some experimental validations were performed and contrasted with the recently acquired outcomes, as shown in Fig. 3. In this semiconductor, low-temperature material consisting of Bi_2Te_3 as *p*- and *n*-type material varies with a temperature difference of 5 to 50 K. The copper electrode properties were largely similar, with no difference in the range of temperature studied. The temperature difference was performed between the bottom and top of the TEG. The bottom temperature was kept at room temperature and the top at a constant temperature in each simulation. Still, it varies with temperature, and all other surfaces are electrically and thermally isolated. Figure 3a shows the electrical potential as a function of temperature difference, known as temperature gradient, obtained at the probe points, and situated in the center of the legs. Therefore, the results are inconsistent with the expected behavior of the electric potential relation (Seebeck coefficient); the results are in the range 50 mV to 1000 mV for a constant temperature difference of 5 K to 50 K.[18] The acquired electrical potential behavior arises from the variation in the effective temperature difference, which increases with the expanding temperature range until it reaches the applied value. According to Eq. (4), the maximum output power is obtained; in this scenario, the device is considered an ideal case. As displayed in Fig. 3b, the temperature distribution of the TEG legs is studied when a consistent temperature difference is applied towards power generated, ranging from 1 mW to 150 mW.

On the other hand, there is no single material thermally stable in the entire temperature regime. In this scenario, there might be a possibility to utilize two or more TEG materials to achieve higher performance; this phenomenon is known as a segmented TEG[16] and is shown in Fig. 1c. As discussed earlier, low-temperature or room-temperature Bi_2Te_3 will be selected for the high figure of merit. Interestingly, this combination of materials is thermally stable for the high-temperature regime, but other material combinations can also be used. As depicted in Fig. 1c, the segmented TEG consists of *p*-type Bi_2Te_3 stacked with Sb_2Te_3 and *n*-type Bi_2Te_3 stacked with PbTe joined thermally in parallel and electrically in series for the maximum power. It can be seen that although the segmented TEG has the highest efficiency at that load resistance, the voltage is almost the same as that of a conventional TEG, as shown in Fig. 4a. Furthermore, Fig. 4b clearly shows that the significance of a segmented TEG is the maximum efficiency with optimum load resistance, and output power is higher than a conventional TEG due to a larger temperature difference.

One of the most effective ways to improve TEG efficiency for their widespread adoption is to follow a hybrid TEG design using Bi_2Te_3, Sb_2Te_3, and PbTe, as shown in Fig. 1d. Interconnected Sb_2Te_3 and Bi_2Te_3 or Bi_2Te_3 and PbTe or Sb_2Te_3 and PbTe TEG legs through a copper electrode will increase the overall electrical resistance of the TEG system. However, the thin film of contact resistance concerning TEG resistance does not always affect the efficiency of the hybrid TEG such as Bi_2Te_3, Sb_2Te_3, and PbTe configure the design where the thermal power under load and unload conditions with the n values defines the efficiency of the TEG as per Eqs. (2) and (3). Therefore, there is no negative effect in the TEG configuration's thermal performance between TE elements and contacts, which provides the enhanced TEG performance, as shown in Fig. 5. For the hybrid TEG system, we examined the trend between the temperature gradient and the

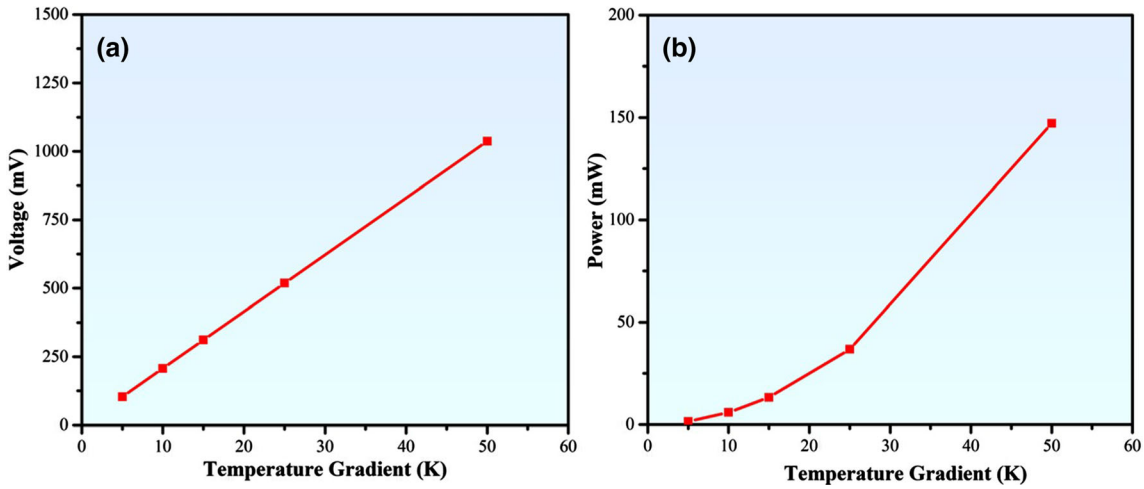

Fig. 3. Conventional TEG system: (a) electrical potential and (b) power as a function of the temperature gradient.

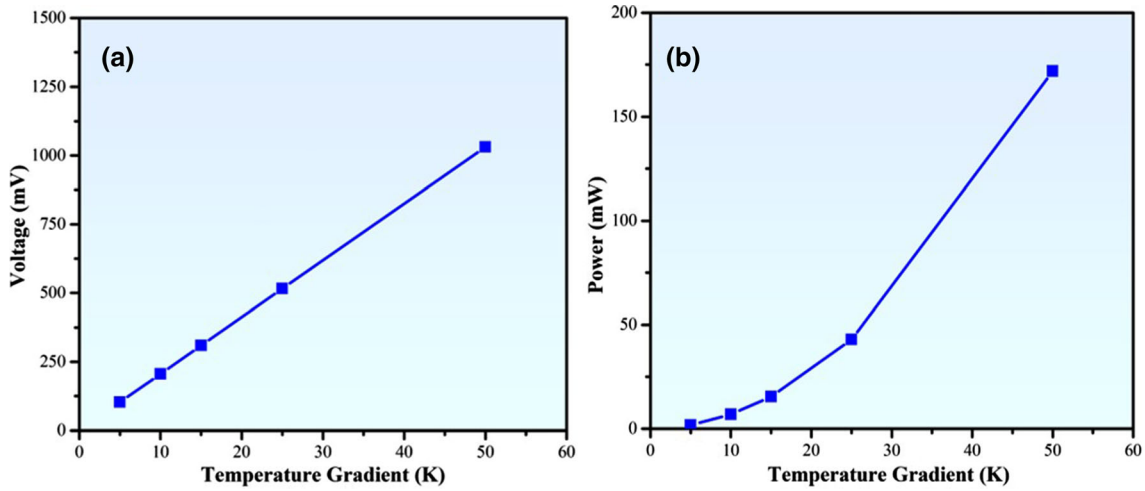

Fig. 4. Segmented TEG system: (a) electrical potential and (b) power as a function of the temperature gradient.

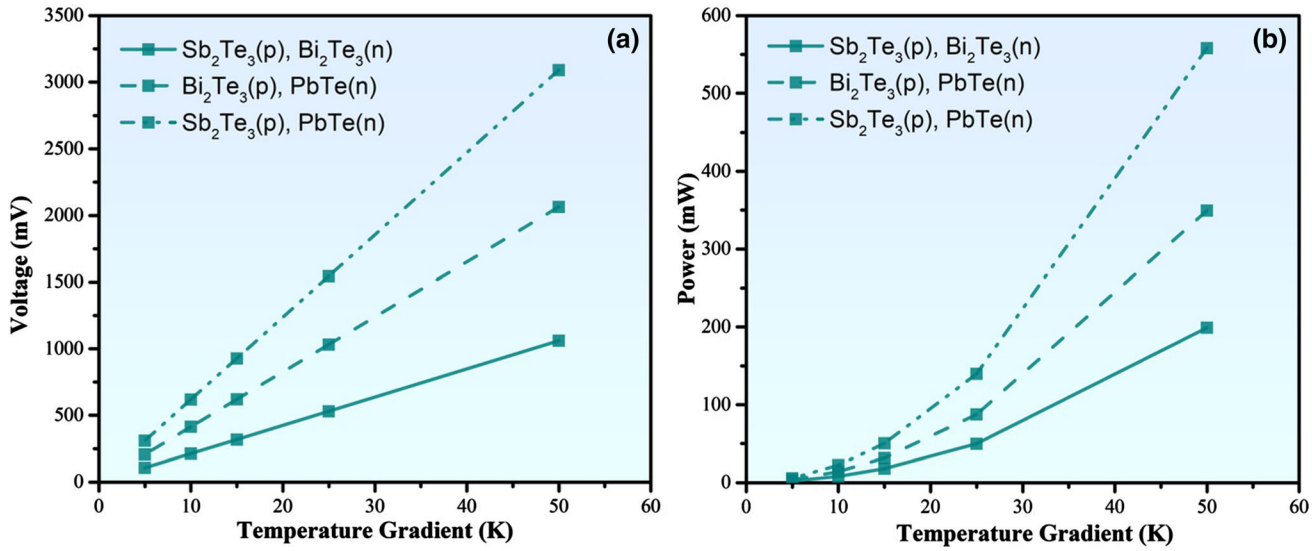

Fig. 5. Hybrid TEG system: (a) electric potential and (b) power as a function of the applied temperature difference.

electrical potential or power. Whenever the electrical potential of voltage increases towards the temperature gradient increase, notably, our module of Sb_2Te_3 and PbTe with 52 legs is able to generate the maximum output voltage of 3000 mV at a temperature difference of 50 K. We measured the power generation performance of the hybrid TEG system for the temperature gradients of 5 to 50 K, which maximized the output power of the TEG to 550 mW, as shown in Fig. 5b. Thus, wherever a decrease of sufficient temperature along with the device and so increase of temperature gradient, and consequently, it is applied with more absorption of heat. The significant point is that the output of a thermoelectric device output is not independent from the external load; otherwise, the thermoelectric is a reliant source for the open-circuit voltage but certainly to the external load resistance.

Further matching the thermal resistance to mechanical resistance is another necessary step towards optimizing the hybrid TEG system performance over its respective temperature regime, as shown in Fig. 6a. Stress examination is especially critical for the TEG framework, since the introduction of expanding temperatures can cause increased pressure on the legs and the joints. Therefore, it is essential to understand the TEG system's yielding nature and what it is dependent on in order to can assess the most significant burden the TEG system can withstand before the device fails. von Mises stress is developed to measure the maximum force and to predict the material's yield strength under complex loading conditions when equal force is applied on the opposite sides of the TEG systems. The hot intersection of the TEG system observes more stress than the cold junction, and this prompts the finish of that when temperature expands the

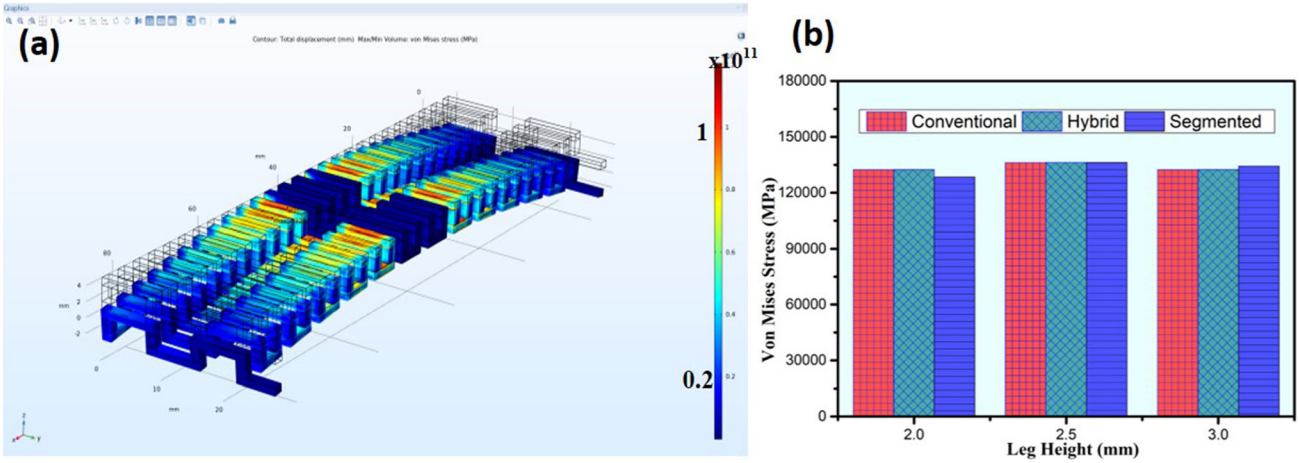

Fig. 6. Nephogram of the von Mises stress of the (a) TEG system, and comparison analysis of the (b) variation of legs as a function of the applied temperature difference.

pressure, similar to the increase in the TEG system when the height ratio is varied. The trend observed during the transient heating of the TEG system of conventional, segmented, and hybrid configurations is shown in Fig. 6b. The benefit of the optimum height ratio for the hybrid system is 0.2 mm while maintaining its enhanced power output compared to the other TEG systems. It can be seen that compared thermal stress in the optimized TEG geometry with lower von Mises stress can increase the lifetime of the TEG system. The von Mises stress of conventional, segmented, and hybrid TEG systems is analyzed; in addition, the outcomes are evaluated. The obtained results are from the optimized length at 2 mm. The conventional, segmented, and hybrid TEG systems indicated the highest yields of 147.122 mW, 171.934 mW, and 550 mW, respectively, at the temperature difference of 50 K.

CONCLUSION

In this paper, a comprehensive numerical in-depth analysis of conventional, segmented, and hybrid TEG systems is presented. The performance of the developed 3D TEG system with the thermal, electrical, and mechanical responses in the form of thermal conductivity, electrical conductivity, Seebeck effects, and von Mises stress is reported. The high-performance hybrid TEG developed in this work reduces mechanical stress through optimization of legs. When a temperature gradient of 50 K for TEG analysis was obtained, power yields of 147.122 mW, 171.934 mW, and 550 mW were achieved for the conventional, segmented, and hybrid TEG systems, respectively.

ACKNOWLEDGMENTS

The authors would like to thank the Visvesvaraya PhD Scheme for Electronics and Information Technology (VISPHD-MEITY2821) and the Innovation in Science Pursuit for Inspired Research (INSPIRE) Faculty Program through the Department of Science and Technology (DST) funded by the Ministry of Science and Technology (DST/INSPIRE/04/2017/002629).

CONFLICT OF INTEREST

The authors declare that they have no conflict of interest.

REFERENCES

1. Y. Liang, C. Zhao, Y. Yuan, W. Zhang, J. Huang, D. Yu, Y. Liu, M.M. Titirici, Y. Cheuh, H. Yu, and Q. Zhang, *Inf. Mat.* 1, 6–31 (2019).
2. K.C. Wilsonab, E. Manikandana, M. BasheerAhameda, and B.W. Mwakikungac, *J. Alloys. Compd.* 585, 555 (2014).
3. K. Kaviyarasu, E. Manikandan, J. Kennedy, M. Jayachandran, and M. Maaza, *Adv. Mater. Lett.* 7, 684 (2016).
4. V. Pandiyarasan, S. Suhasini, K. Faizan, G. Aranya, A. Majumdar, H. Yasuhiro, and I. Hiroya, *Carbohydr. Polym.* 157, 1801 (2017).
5. S. Suhasini, G. Greeshma, K. Prashanth, V. Kathirvel, T.S. Saranya, V. Pandiyarasan, D.W. Karolien, and H. Ikeda, *Appl. Surf. Sci.* 449, 513 (2018).
6. H. Chen, N.C. Thang, Y. Wei, C. Tan, Y. Li, and Y. Ding, *Prog. Nat. Sci.* 19, 291 (2009).
7. V. Pandiyarasan, S. Suhasini, G. Thanga, K. Jayabal, R. Kumar, K. Denis, and I. Hiroya, *Appl. Surf. Sci.* 496, 143658 (2019).
8. V. Pandiyarasan, S. Suhasini, H.C. Kalari, M. Omprakash, K. Karthikeyan, T. Tsunehiro, and I. Hiroya, *J. Alloys Compd.* 695, 888 (2017).
9. C. Hyeongdo, J.K. Yong, S. Jinseob, S.K. Choong, S.L. Gyu, K. Seongho, P.K. Jiwon, Y. Hwan, H.P. Sang, H. Hye Rim, H. Min-Hee, V. Pandiyarasan, and J.C. Byung, *Adv. Funct. Mater.* 29, 1901505 (2019).
10. T.S. Ferreira and A.M. Pereira, *Energy Convers. Manag.* 169, 217 (2018).
11. C. Daniel, *Energy Convers. Manag.* 140, 167 (2017).
12. C. Zhi-Gang, H. Guang, Y. Lei, C. Lina, and Z. Jin, *Prog. Nat. Sci.* 22, 535 (2012).
13. S. Yongming, Z. Zhixiang, D. Yuan, Z. Wei, C. Xin, and Z. Yongsheng, *Energy Convers. Manag.* 101, 713 (2015).
14. S. Samson, L. Guiqiang, Z. Xudong, M. Xiaoli, G.A. Yousef, and A. Emmanuel, *Energy Convers. Manag.* 184, 180 (2020).
15. H. Constantinos, K. Elias, and G. Julius, *Energy Convers. Manag.* 66, 165 (2013).

16. S. Samson, L. Guiqiang, Z. Xudong, M. Xiaoli, G.A. Yousef, and A. Emmanuel, *J. Power Sour.* 53, 428 (2019).
17. J. Nesrine, B. Ayda, M. Jens, M. Brahim, T. Fares, and I. Mohammed, *Energy Rep.* (2019). https://doi.org/10.1016/j.egyr.2019.12.011.
18. H. Xiaokai, T. Hiroyuki, N. Kazuo, O. Michihiro, and Y. Atsushi, *J. Electron. Mater.* 44, 3637 (2015).
19. H. Ikeda, K. Faizan, V. Pandiyarasan, S. Shota, N. Mani, S. Masaru, M. Kenji, and H. Yasuhiro, *J. Phys: Conf. Ser.* 1052, 12017 (2018).